

# Polyrotaxane/DNA Conjugate by Use of Intercalation: Bridge Formation between DNA Double Helices

Kenji Tokuhisa, Emi Hamada, Ryouji Karinaga, Naohiko Shimada, Yoichi Takeda, Shinichi Kawasaki,<sup>†</sup> and Kazuo Sakurai\*

Department of Chemical Processes & Environments, The University of Kitakyushu, 1-1 Hibikino, Wakamatsu-ku, Kitakyushu, Fukuoka 808-0135, Japan, and Advanced Material Business Promotion Department, Osaka Gas Co., Ltd. 6-19-9, Torishima Konohana-ku, Osaka 554-0051, Japan

Received February 25, 2006; Revised Manuscript Received October 31, 2006

**ABSTRACT:** Fluorene has been known as an intercalator of DNA. This paper shows that the fluorene–DNA interaction has a relatively large binding constant (ca.  $10^{7-8} \text{ M}^{-1}$  at least larger than  $10^6 \text{ M}^{-1}$ ). This large binding constant is consistent with the experimental fact that adding fluorenone stoichiometrically ejects the ethidium bromide that had been beforehand intercalated in DNA. A polyrotaxane was made from polyethylene glycol and  $\alpha$ -cyclodextrin, and the both ends were capped with fluorene (dF-CD-PEG). When we mixed dF-CD-PEG and DNA, atomic force microscopy showed that the DNA was interlinked with dF-CD-PEG. The present work proves that DNA intercalators can be useful for a building block to manipulate DNA when they are combined with polyrotaxanes.

## Introduction

Supramolecular chemistry has a unique strategy to build up molecules to nanoscopic assembly using hydrogen bonds, metal coordination, and inclusion phenomena of calix[n]arenes and cyclodextrins.<sup>1,2</sup> One of the characteristics is not to use covalent bonds, therefore, which should provide dynamics and flexibility to the assembly. Supramolecular chemistry is now merging with macromolecular chemistry to yield a new field that can be called “supermacromolecular” chemistry.<sup>3</sup> DNA certainly should be a central player in this field, and the DNA-related supermacromolecular chemistry contains great potential in practical applications such as gene delivery or DNA sequence sensing. The present paper demonstrates that DNA intercalators can be a useful building block or tool to manipulate DNAs when they are combined with polyrotaxanes.

Intercalators are compounds that can slide into the gaps between DNA bases.<sup>4,5</sup> Upon intercalation, DNA conformation is dramatically altered and generally becomes rodlike due to increasing the chain stiffness.<sup>6</sup> The essential structural feature for the intercalators is possession of an extended planar heteroaromatic ring, typically three fused six-membered rings. Ethidium bromide (EtBr) is the most commonly used intercalator. EtBr displays a loss of optical density (hypochromicity) as well as a dramatic increment of its fluorescence intensity when EtBr slips between two base pairs of DNA.<sup>7</sup> The maximum number of intercalators that can bind to the DNA helix is one intercalator versus two base pairs. This “neighbor-exclusion principle” is one of the characteristic features of the DNA intercalators.<sup>8</sup>

Fluorene is a tricyclic aromatic hydrocarbon and contains a five-membered ring. Fluorene seems to perfectly possess structural requirements for DNA intercalators; however, to the best of our knowledge, there has been a few reports for intercalating fluorene into DNA, except for tilorone (2,7-bis[(diethylamino)-

ethoxy]-fluorene-9-one)<sup>5,9</sup> and 9-fluorene- $\beta$ -O-glycoside<sup>10</sup> and its analogues. Fluorene is a major component of fossil fuels and their derivatives and is also a byproduct of coal conversion. The 9th carbon of fluorine is relatively more active than the other carbons, and thus it is easy to convert fluorene to fluorenone. Many chemical techniques are available to attach functional groups to the carbonyl group of fluorenone, including alkyl chains or polyethylene glycols (PEG).

Harada et al.<sup>11–13</sup> extensively studied a series of polyrotaxanes made from cyclodextrins (CD) and polyethylene glycol (PEG).  $\alpha$ -CD can include PEG chains to form polyrotaxanes when they are mixed in aqueous solutions. When both ends of the PEG were capped by 9-anthryl groups,  $\alpha$ -CD molecules did not form polyrotaxanes because  $\alpha$ -CD cannot go through the anthracene moiety.<sup>14</sup> On the other hand, the 9-anthryl group capping was made after the  $\alpha$ -CD/PEG polyrotaxane complex was formed; the  $\alpha$ -CD molecules were trapped on the PEG chain and never escaped from it. The fully  $\alpha$ -CD loaded polyrotaxane shows a rodlike nature so that it is easy to observe the architecture with electron microscopy.<sup>15</sup>

Our basic idea is that the fluorene or anthracene that are capping the end of the polyrotaxanes can be used as an intercalator. If so, these polyrotaxanes can bind to DNA to change the DNA conformation.

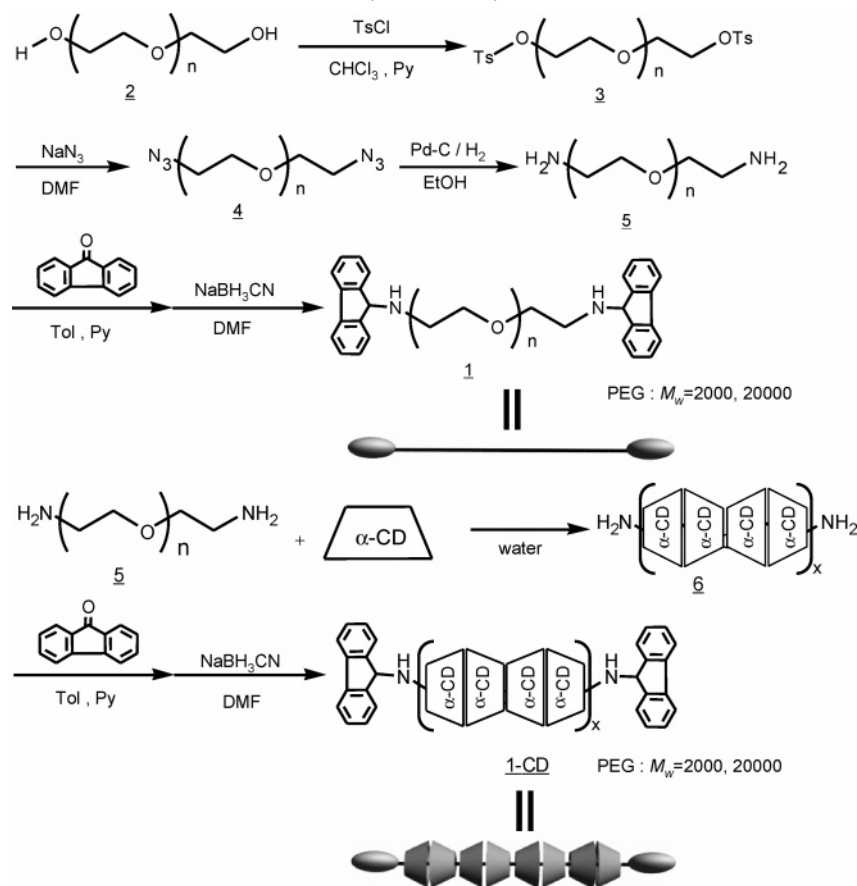
## Experimental Section

**Materials.** Fluorene, PEG ( $M_w = 2000$  or  $20\,000$ ), and  $\alpha$ -CD was purchased from Wako (Japan), and salmon sperm DNA was purchased from Amersham Biosciences (Japan). The molecular weight distribution ( $M_w/M_n$ ) of PEG was less than 1.1. Three fluorene derivatives; 9,9-dimethylfluorene(b), 3,6-dicyano-9,9-dimethylfluorene(c), and 9,9-bis-phenylsulfanyl-fluorene(d) (b, c, and d in Figure 2, respectively) were kindly supplied by Osaka Gas (Japan). Here,  $M_w$  and  $M_n$  are the weight- and number-averaged molecular weights, respectively, determined with gel permeation chromatography.

**Preparation of the Linear-Stranded DNA with the Same Contour Length.** Plasmid DNA of pEGFP-C1 (4731bp BD Biosciences Clontech) was amplified with *E. coli* XL-1 and extracted with a HiSpeed Plasmid Maxi Kit (QIAGEN). The

\* Corresponding author. E-mail: sakurai@env.kitakyu-u.ac.jp. Telephone: +81 93-695-3298. Fax: +81-93-695-3390.

<sup>†</sup> Advanced Material Business Promotion Department, Osaka Gas Co., Ltd..

**Scheme 1. Synthetic Procedure of Fluorene-capped Polyethylene Glycol (dF-PEG) and Fluorene-capped  $\alpha$ -CD/PEG Polyrotaxane (dF-CD-PEG)**

resultant pEGFP-C1 was cleaved with a restricted enzyme Dra III (Bio Labs). This restricted enzyme cuts pEGFP-C1 in only one position. Therefore, the resultant DNAs have the same length. This was confirmed by gel electrophoresis, and this DNA sample was denoted by dpDNA.

**Measurements of Atomic Force Microscopy (AFM).** A dilute solution (final concentration of DNA were about 2 ng/ $\mu$ L) containing 2 mM MgCl<sub>2</sub> was cast onto a piece of freshly peeled mica. The mica surface was washed with distilled water at least ten times. The mica specimen was dried by placing in a vacuum desiccator. The details were described in elsewhere.<sup>16,17</sup> AFM imaging was performed in an AC mode with JSPM-5200 (JEOL). We measured the end-to-end distance for the intercalated DNA with fluorene. To check the reproducibility of the AFM images, we prepared the DNA samples twice, repeating every procedure including the DNA amplification, and four or five AFM specimens were prepared for each condition. In some cases, many DNA molecules were attached in some part of the specimen (or sometimes entire specimen), and thus we could not measure the length. For these cases, we did not include them in the measurements.

**Spectroscopy.** Circular dichroism (CD) and fluorescence spectroscopy were measured with a Jasco J-720WI spectropolarimeter with a 1.0 cm cell and a Hitachi F-4500, respectively. The detailed experimental procedures were described elsewhere.<sup>16</sup>

**Synthesis of Polyethylene Glycol Diamine (5).** The synthetic scheme is presented in Scheme 1. PEG (20 mg, 0.01 mol,  $M_w = 2000$ , 2) was dissolved in 250 mL of chloroform, and 50 mL of pyridine was added to the solution. Under stirring at about 0 °C, 5.4 g of *p*-toluenesulfonate (0.028 mol, 3 times molar of PEG) was added, and after stirring for 3 h, a large amount of cold water was added to terminate the reaction. After lyophilization, the reactant was purified with silica gel (Wako, C-300) gradient chromatography using chloroform/ethanol. The purified solution was lyophilized to obtain the product 3 (yield 86%, 19.8 mg). Product 3 (19.8 mg) was dissolved in 200 mL of DMF, 1.68 mg of sodium azide was

added to the solution, and the reaction was carried out at 80 °C for 24 h. The reactant was dissolved in a large amount of acetone, and the solution was filtered and lyophilized to obtain the product 4 (14.28 mg). The 300 mL ethanol solution of 4 in an autoclave (TAIATSU TECHNO CORP, 1000 mL) was catalytically reduced with 200 mg of palladium carbon for 60 °C for 48 h. The reactant was filtered, lyophilized, and purified with silica gel (Wako, C-300) gradient chromatography using chloroform/ethanol to obtained 5 (yield 58%, 8.3 mg). By use of PEG with  $M_w = 20\,000$ , we prepared another polyethylene glycol diamine with the similar method.

**Synthesis of Fluorene-Capped PEG (1) and Polyrotaxane (1-CD).** As presented in Scheme 1, 8 mg of fluorenone and 5 mL of pyridine were added to the 8.3 mg of 5 ( $M_w$  of PEG = 2000) toluene solution, and the solution was stirred for about 3 days. After toluene was removed by evaporation, the product was diluted with 50 mL of DMF, sodium cyanoborohydride (excess) was added, and the mixture was stirred for 4 days. The reactant was purified with silica gel (Wako, C-300) gradient chromatography using chloroform/ethanol and Sephadex-LH20 to obtain 1 (6.17 mg). In a similar manner, we made 1 with  $M_w$  of PEG = 20 000. These samples were denoted by dF-PEG2000 and dF-PEG20000, corresponding to the PEG chain length, respectively.

$\alpha$ -CD (10 mg) was added to 9.8 mg of 5 ( $M_w$  of PEG = 2000) in 100 mL of water. After stirring for 24 h, a white precipitant was formed. The precipitant was collected and dissolved in DMSO, and 1.8 mg of fluorenone was added. Reductive amination was carried out in a similar manner to that mentioned above to obtain 1-CD. In a similar manner, we made CD-1 with  $M_w$  of PEG = 20 000. These samples were denoted by dF-CD-PEG2000 and dF-CD-PEG20000. <sup>1</sup>H NMR was performed to assign the chemical structure of the products with a LNM-ECP500 at the Instrumentation Center of the University of Kitakyushu.

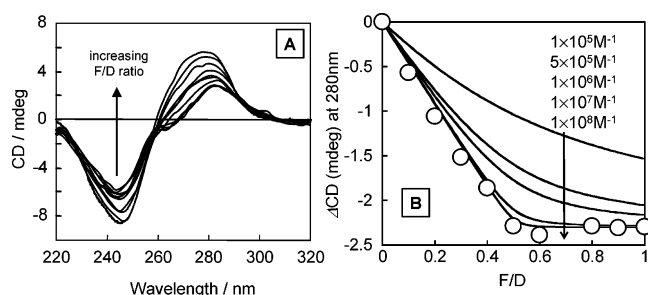


**Figure 1.** (A) Changes of circular dichroism (CD) when fluorene was added to DNA in a water/THF (1:1 volume) solution. The  $F/D$  ratio was changed from 0 to 1.0. (B) The change of CD at 280 nm was plotted against  $F/D$ , compared with the theoretical values with the different binding constants; from top:  $K_b = 1 \times 10^5$ ,  $5 \times 10^5$ ,  $1 \times 10^6$ ,  $1 \times 10^7$ , and  $1 \times 10^8$   $M^{-1}$ , respectively.

## Results and Discussion

**Intercalation of Fluorene into DNA: Spectroscopy.** Figure 1A shows the CD spectral changes when fluorene was added to salmon sperm DNA in a tetrahydrofuran (THF)/water (1:1 volume) solvent. With increase of the fluorene/DNA molar ratio ( $F/D$ ), the CD magnitude decreases at both positive (280 nm) and negative (245 nm) bands. These changes seem saturated at higher  $F/D$  values. Figure 1B plots the difference of the CD intensity ( $\Delta CD$ ) at 280 nm against  $F/D$ , where  $\Delta CD$  was obtained by subtracting the CD value at  $F/D = 0$  from the observed one for each  $F/D$ . There is a clear turnoff point at  $F/D = 0.5$ , indicating that two base pairs versus one fluorene are the constitutional unit of this interaction. This stoichiometric number agrees with the neighbor-exclusion principle of intercalators. The solid lines in panel B presents the theoretical values, which were calculated on the assumption that the chemical equilibrium is held between DNA and fluorene and the equilibrium binding constant ( $K_b$ ) is a function of only the concentrations of them. The data points can be fitted by the theoretical line with a  $K_b$  value ranging between  $10^8$  and  $10^7$   $M^{-1}$ . The resultant  $K_b$  of fluorene seems relatively large compared with those of other intercalators.<sup>17</sup>

Because the solubility of fluorene in water is considerably low (ca. less than  $10^{-5}$  M), we could not use pure water as the solvent; thus, we used a THF/water (1:1 volume) mixture as the solvent. There is a possibility that the mixed solvent might increase the binding constant. Nevertheless, this is unlikely because DNA intercalation is generally driven by hydrophobic interactions and hydrophobic interactions should become less favorable in mixed solvents compared with those in pure water. Fluorene derivatives such as tilorone (2,7-bis[(diethylamino)-ethoxy]-fluoren-9-one)<sup>5,9</sup> and 9-fluoren- $\beta$ -O-glycoside<sup>10</sup> have been known to intercalate DNA. Anthracene derivatives, which have similar structures with fluorene, are also an intercalator.<sup>18</sup> Their  $K_b$  values range around  $10^5$ – $10^6$   $M^{-1}$ , much smaller than that of fluorene estimated above. By the way, when we carried out the same experiment for fluorenone, we obtained the same results as those in Figure 1, showing that  $K_b$  of fluorenone is also in the range of  $10^8$ – $10^7$   $M^{-1}$ , at least more than  $10^6$   $M^{-1}$ .

EtBr exhibits a tremendous increment in fluorescence emission upon intercalation and its  $K_b$  is about  $10^5$   $M^{-1}$  in water.<sup>7</sup> When we added fluorenone to a salmon sperm DNA aqueous solution, where the salmon sperm DNA had been intercalated with EtBr beforehand, the EtBr originated fluorescence was drastically reduced, as presented in Figure 2A. This is because fluorenone competed with EtBr in intercalating DNA and overwhelmed it. Here, we used fluorenone instead of fluorene because the fluorescence inherent in fluorene made accurate

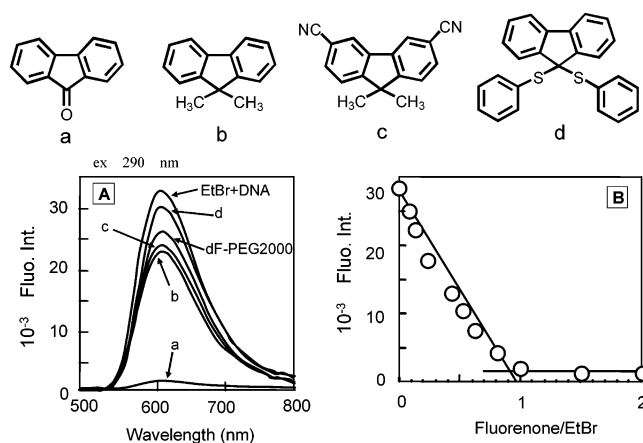


**Figure 2.** (A) Decrease in the EtBr fluorescence intensity (excited at 290 nm) when fluorenone and three derivatives were added at the same molar amount of EtBr. (B) The fluorescence intensity at 605 nm plotted against the fluorenone/EtBr molar ratio.

measurement difficult. Owing to the low concentration of EtBr (ca.  $10^{-6}$  M) available to measure fluorescence, we could carry out this experiment in water. Figure 2B plots the EtBr fluorescence intensity against the fluorenone/EtBr molar ratio, showing that the EtBr fluorescence completely disappeared when fluorenone was added in an equal amount of EtBr. This means that added fluorenone completely ejected EtBr and intercalated into DNA, indicating that the binding constant of fluorenone is one or more orders larger than EtBr. This result is consistent with that of Figure 1, confirming the considerably large  $K_b$  of fluorenone (probably the same as fluorene) in water.

When a fluorene derivative in which the 9th position was substituted with a dimethyl group (b in Figure 2) was added to the same EtBr-intercalated salmon sperm DNA solution, the fluorescence intensity was decreased by about 30%. This means that the binding constant of compound b is smaller than that of fluorenone. However, the substitution of the 3rd and 6th positions did not decrease the binding constant so much. When a bulky group was attached at the 9th position (d in Figure 2), the decrease of the intensity was less than 10%, suggesting that the binding constant of compound d is less than  $10^5$   $M^{-1}$ . When we carried out the same experiments with dF-PEG or dF-CD-PEG, the intensity was also decreased by about 25%, as shown in the Figure 2. These results indicate that the end-capping fluorene can intercalate DNA, although the  $K_b$  is less than that of fluorene or fluorenone. The decreased  $K_b$  can be ascribed to the attachment of water-soluble PEG chain as well as the steric hindrance of the 9th position.

**Intercalation of Fluorene into DNA: Microscopy.** Figure 3 shows the AFM images when we added fluorene to dpDNA. Here, all DNA molecules should have the same contour length because we prepared dpDNA by cleaving the amplified plasmid DNA of pEGFP-C1 with a restriction enzyme, Dra III. This fact was confirmed with gel electrophoresis (see the Supporting Information Figure 2S) and AFM observation (Table 1). As presented in Figure 3, addition of fluorene resulted in changes in the DNA conformation and DNA chains were considerably extended. As shown by the bar chart, although there is large experimental error, the averaged end-to-end distance was increased with increasing  $F/D$ . This trend is beyond the experimental error, as indicated by t-test. The result indicates the increment of the chain stiffness of DNA with increasing  $F/D$ . The feature observed in the figure agrees with the general results for DNA intercalation.<sup>17</sup> The upper inset plot shows the surface height along the white bar of image A. The height of



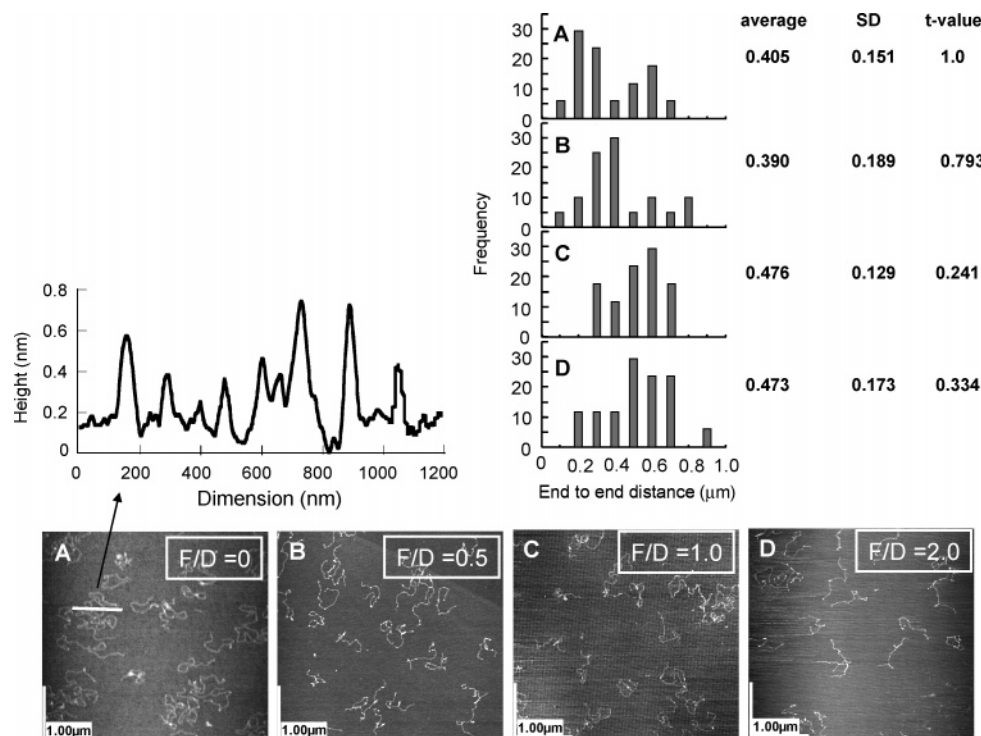


**Figure 3.** AFM observation for the dpDNA intercalated with fluorene at  $F/D = 0, 0.5, 1.0$ , and  $2.0$ . The upper inset show the height distribution along the white line drawn in image A, and the bar charts represent the end-to-end distance distributions for the four images as well as the averaged values, the standard deviations, and the t-test values.

**Table 1. Numerical Results of AFM**

	dpDNA	$\alpha$ -CD	dF-CD-PEG20000
height/nm	$0.76 \pm 0.05$	$0.62 \pm 0.05$	$0.67 \pm 0.05$
contour length/nm	$1700 \pm 100$		$150 \pm 30$
	$1622^a$		$160^b$

<sup>a</sup> Calculated from 10.5 bases or 3.6 nm per turn (Lehninger, A. L.; Nelson, D. L.; Cox, M. M. *Principles of Biochemistry*; W. H. Freeman: New York, 2004; Chapter 10, p 336) and 4731 base pairs of dpDNA

<sup>b</sup> Based on 0.36 nm for the fully extended PEG unit.

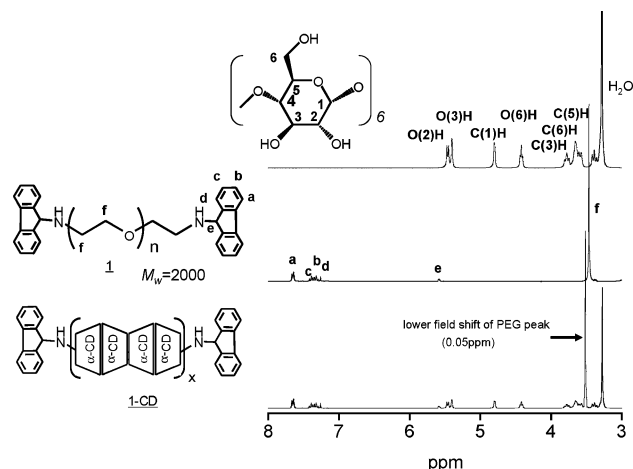


**Figure 4.**  $^1\text{H}$  NMR spectra of  $\alpha$ -CD, dF-PEG2000, and dF-CD-PEG2000. The numerically and alphabetically marked peaks correspond to  $\alpha$ -CD and fluorene, respectively. The ethylene peak in PEG was shifted toward the lower field upon the polyrotaxane formation.

DNA ranges 0.6–0.8 nm, and these values are much smaller than the diameter of DNA (2.0 nm at dry state). Lower heights than real objects are often observed with AFM after the mica surface was washed with water.

**Synthesis of dF-PEG (1) and dF-CD-PEG (1-CD).** Fluorene-capped polyethylene glycol has been prepared according

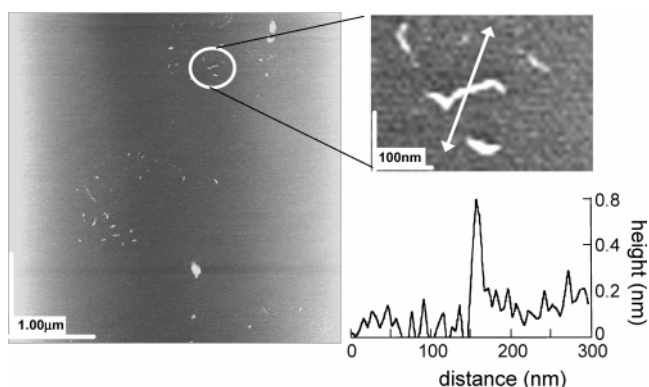


**Figure 5.** AFM observation for dF-CD-PEG2000. One rod-like image was magnified, and the height was measured along the line.

to the procedure presented in the upper part of Scheme 1. Figure 4 shows the typical  $^1\text{H}$  NMR spectrum for dF-PEG2000. All of the peaks can be assigned as presented in the figure, and the integrated intensity ratios of the peaks were consistent with the chemical structure, indicating that the two PEG ends were capped by fluorene.  $^1\text{H}$  NMR spectrum for dF-PEG20000 had very small fluorene-oriented peaks (see the supplementary) owing to the dominant amount of PEG, causing no obtaining of an accurate intensity ratio of the PEG to fluorene moieties. However, we can presume that the majority of the compounds have capped fluorene at both ends because the synthetic procedure was the same as that of dF-PEG2000.

Figure 4 also shows the  $^1\text{H}$  NMR spectrum for dF-CD-PEG2000. As reported by Harada et al.,<sup>14</sup> upon the formation of the inclusion complex from PEG and  $\alpha$ -CD, the methylene peaks shift by 0.05 ppm to the lower magnetic field. There is a small amount of unshifted methylene peaks observed in Figure 4B, and the intensity ratio of the unshifted to shifted peaks is less than 5%. This fact indicates that most of the PEG chain is included in  $\alpha$ -CD. This concludes that we obtained a

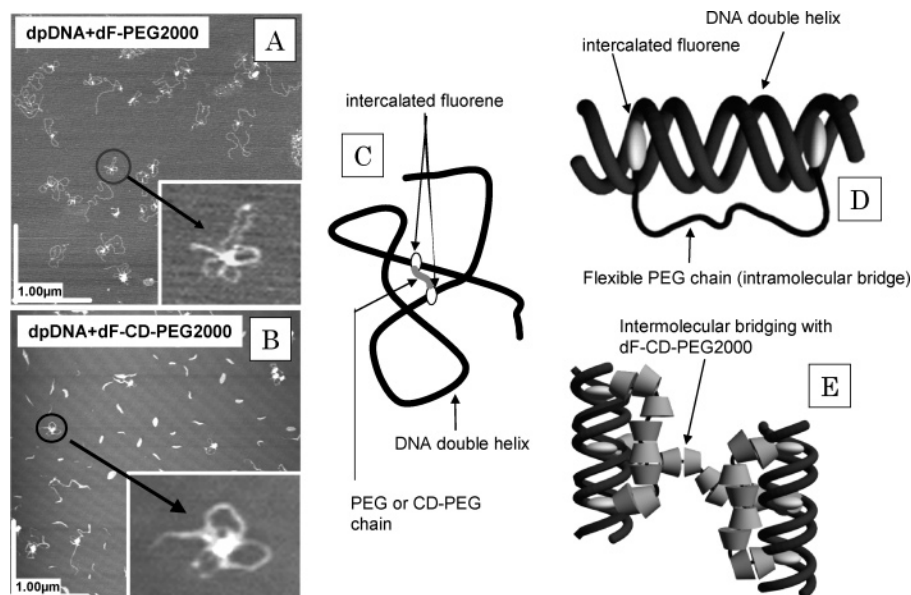


**Figure 6.** Typical AFM images for the mixtures of dpDNA+dF-PEG2000 (upper) and dpDNA+dF-CD-PEG2000 (lower) and the magnification of the images. The left illustrations show how the images can be interpreted.

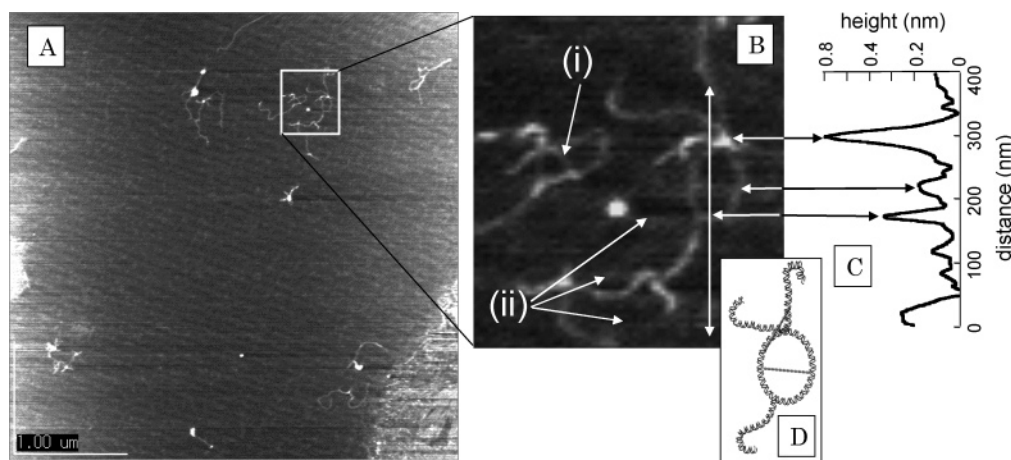


**Figure 7.** Typical AFM image for the mixtures of dpDNA+dF-PEG2000 and its magnification (A and B). The height of the image was measured along the white bar (C). The inset illustration (D) shows how dpDNA and dF-PEG2000 are connected to show the magnified image. In the B image, (i) shows another example of the bridging and (ii) shows artificial images.

fluorene-capped polyrotaxane, as schematically presented in Scheme 1.

**Conjugation between dF-CD-PEG and DNA.** Figure 5 shows an AFM image for dF-CD-PEG20000, showing that rodlike architectures are scattered on the mica surface. The height of the image was evaluated to be  $0.67 \pm 0.05$  nm after averaging more than 10 objects (see Table 1). This value smaller than the diameter of  $\alpha$ -CD (ca. 1.5 nm), however, agrees with those observed for polyrotaxanes in the previous studies.<sup>15</sup> This discrepancy can be explained by the same reason for water-washed mica mentioned above. The contour length of this rodlike image is 180 nm, consistent with the value (160 nm) estimated from the fully extended PEG chain length. The averaged length of the rodlike image including other samples was  $150 \pm 20$  nm. When we observed dF-PEG20000 with AFM, there were only dots. This can be ascribed to the flexibility of the PEG chain, probably causing gathering of the segments and the fluorene moieties attached at the both ends. dF-PEG2000 and dF-CD-PEG2000 did not show any significant images because of the short chain length of the PEG (ca. 16 nm).

We always observed the clusterlike images, whose lengths were shorter than the fully extended dF-CD-PEG20000 and

whose heights were much larger than the expected diameter of  $\alpha$ -CD. When the heights were more than 1.0 nm, we excluded them from the counting. We observed these images only when we examined the cyclodextrins–polyrotaxane. We suppose that these images were made from bent dF-CD-PEG20000 and aggregates of them, or simply from aggregate of CDs themselves.

We carried out AFM observation for the mixtures of dF-CD-PEG2000 (or dF-PEG2000) and dpDNA at various  $F/D$  ratios. When the  $F/D$  ratio was lower than 2, any appreciable change was not observed for the conformation of dpDNA. On the other hand, in the case of mixing with fluorene, the DNA conformation was extended in the range of  $F/D > 1$  (Figure 3). This difference may be related the difference in the binding constant between fluorene and dF-PEG2000 (see Figure 2A), i.e., the binding constant of dF-CD-PEG2000 (or dF-PEG2000) is smaller than that of fluorene. To induce the conformational changes, we had to add dF-CD-PEG2000 (or dF-PEG2000) more than  $F/D = 2$ .

Parts A and B of Figure 6 show the AFM images after mixed with dF-PEG2000 (A) and dF-CD-PEG2000 (B) with dpDNA at  $F/D = 2$ , respectively. The addition of both dF-PEG2000

and dF-CD-PEG2000 led the DNA molecules to partially aggregate with each other. They were bound at a certain points, seemingly to form a flowerlike architecture. The high of the junction points were about 2 nm for dF-PEG2000 and 4 nm for dF-CD-PEG2000, suggesting that a few DNA chains were stacked with each other at this point. It should be emphasized that these bundled DNA were more frequently observed when we added dF-PEG2000 or dF-CD-PEG2000, compared with dpDNA itself and fluorene-added dpDNA (Figure 3). These results can be explained by the fluorene moieties at both ends of the dF-PEG2000 or dF-CD-PEG2000 intercalating dpDNA to result in forming the inter- or intramolecular bridge between DNAs (D and E), as schematically illustrated in the figure, and the resulting bridge should lead to flowerlike architecture as presented in (C).

When we added dF-CD-PEG20000 to dpDNA, characteristic AFM images were observed (Figure 7). The difference between Figures 6 and 7 is that a short rod (with a length of about 150 nm) connects the dpDNA, as presented in the magnified images (panel B). When we measured the height of the rods, the averaged value was 0.67 nm, which is almost equal to that of dF-CD-PEG20000 itself (panel C). The contour length of the short rod also agreed with that of dF-CD-PEG20000 itself. Consequently, the characteristic feature in the panels A and B of Figure 7 can be interpreted by assuming that the fluorene moieties at both ends of the dF-CD-PEG20000 intercalate dpDNA and the stiff polyrotaxane appears as a rod connecting DNA, as schematically illustrated in Figure 7D.

We have to accept that there is ambiguity in interpreting the AFM images in Figure 7, and the microscopic data was not enough to lead firm conclusions. One reason for the ambiguity should be that AFM observation was carried out for ultradiluted conditions (2 ng/ $\mu$ l of DNA and the mica surface was washed with distilled water at least ten times), which should change the number of the intercalated fluorene. Another reason is that, because  $\alpha$ -CD can include fluorene,<sup>19</sup> the fluorene moieties at the end of dF-CD-PEG can be included by  $\alpha$ -CD and reduce activity to intercalate DNA. By the way, when we carried out gel electrophoresis comparing dF-PEG20000+dpDNA with dF-PEG2000+dpDNA (see the Supporting Information S4), dF-PEG20000+dpDNA showed a smear-retarded band and dF-PEG2000+dpDNA showed an advanced band compared with the original dpDNA. We considered that the retarded band can be ascribed to increased molecular mass due to intermolecular bridging and the advanced band can be ascribed to decreased hydrodynamic volume due to intramolecular bridging with the shorter PEG chain. These findings presumably support our conclusions.

## Conclusions

The present work showed that the fluorene–DNA interaction has a relatively large binding constant (ca.  $10^{7-8}$  M<sup>-1</sup>, at least

larger than  $10^6$  M<sup>-1</sup>), and the ethidium bromide beforehand intercalated in DNA can be ejected by adding fluorenone. By applying this advantage to manipulate DNA, we prepared the PEG/ $\alpha$ -CD polyrotaxanes with both end-capped with fluorene (dF-PEG2000 and dF-CD-PEG20000). AFM showed that the DNA was interlinked with the polyrotaxane only when we added dF-CD-PEG20000. The present work proved that DNA intercalators can be a useful building block to manipulate DNAs when they are combined with polyrotaxanes.

**Acknowledgment.** This work is financially supported by JST SORST program and Grants-in-Aid for Scientific Research (16350068 and 16655048). We thank Dr. Lee at the University of Kitakyushu for helpful discussion for AFM. This paper is dedicated to Prof. William J. MacKnight (University of Massachusetts, Amherst, MA) on his 70th birthday.

**Supporting Information Available:** <sup>1</sup>H NMR for dF-CD-PEG20000, gel shift assay to confirm the uniform length of dpDNA, further AFM images to construct the bar chart in Figure 3, gel shift assay for dF-PEG20000+dpDNA and dF-PEG2000+dpDNA. This material is available free of charge via the Internet at <http://pubs.acs.org>.

## References and Notes

- (1) Ikeda, A.; Shinkai, S. *Chem. Rev.* **1997**, *97*, 1713.
- (2) Nepogodiev, S. A.; Stoddart, J. F. *Chem. Rev.* **1998**, *98*, 1959.
- (3) Amabilino, D. B.; Stoddart, J. F. *Chem. Rev.* **1995**, *95*, 2725.
- (4) W. David Wilson, W. D.; Wang, Y. H.; Kusuma, S.; Chandrasekaran, S.; Yang, N. C.; Boykin, D. W. *J. Am. Chem. Soc.* **1985**, *107*, 4989.
- (5) Geller, K.; Reinert, K. E.; Schulze, W. *Biomed. Biochim. Acta* **1985**, *44*, 1095.
- (6) Berge, T.; Jenkins, N. S.; Hopkirk, R. B.; Waring, M. J.; Edwardson, J. M.; Henderson, R. M. *Nucleic Acids Res.* **2002**, *30*, 2980.
- (7) McMurray, C. T.; Van Holde, K. E. *Biochemistry* **1991**, *30*, 5631.
- (8) Kumar, C. V.; Asuncion, E. H. *J. Am. Chem. Soc.* **1993**, *115*, 8547.
- (9) Bischoff, G.; Gromann, U.; Lindau, S.; Skolzig, R.; Witkowski, W.; Bohley, C.; Naumann, S.; Sagi, J.; Meister, W. V.; Hoffmann, S. *J. Biomol. Struct. Dyn.* **2000**, *18*, 199.
- (10) Alcaro, S.; Arena, A.; Neri, S.; Ottana, R.; Ortuso, F.; Pavone, B.; Vigorita, M. G. *Bioorg. Med. Chem.* **2003**, *12*, 1781.
- (11) Harada, A.; Li, J.; Kamachi, M. *Nature* **1992**, *356*, 325.
- (12) Harada, A.; Li, J.; Kamachi, M. *Nature* **1993**, *364*, 516.
- (13) Harada, A.; Li, J.; Kamachi, M. *Macromolecules* **1993**, *26*, 5698.
- (14) Okada, M.; Harada, A. *Macromolecules* **2003**, *36*, 9701.
- (15) Okumura, Y.; Ito, K.; Hayakawa, R.; Nishi, T. *Langmuir* **2000**, *16*, 10278.
- (16) Wu, Y. S.; Koch, K. R.; Abratt, V. R.; Klump, H. H. *Arch. Biochem. Biophys.* **2005**, *440*, 28.
- (17) Neidle, S. *Nucleic Acid Structure and Recognition*; Oxford University Press: New York, 2002.
- (18) Modukuru, N. K.; Snow, K. J.; Perrin, B. S., Jr.; Thota, J.; Kumar, C. V. *J. Phys. Chem. B* **2005**, *109*, 11810.
- (19) Wu, Y.; Ishibashi, K.; Deguchi, T.; Sabemasa, I. *Bull. Chem. Soc. Jpn.* **1990**, *63*, 3450.

MA060419V